

# Addressing Overthinking in Large Vision-Language Models via Gated Perception-Reasoning Optimization

Xingjian Diao<sup>1</sup>, Zheyuan Liu<sup>2</sup>, Chunhui Zhang<sup>1</sup>, Weiyi Wu<sup>1</sup>, Keyi Kong,  
Lin Shi<sup>3</sup>, Kaize Ding<sup>4</sup>, Soroush Vosoughi<sup>1</sup>, Jiang Gui<sup>1</sup>

<sup>1</sup>Dartmouth College, <sup>2</sup>University of Notre Dame, <sup>3</sup>Cornell University, <sup>4</sup>Northwestern University  
xingjian.diao@dartmouth.edu

## Abstract

Large Vision-Language Models (LVLMs) have exhibited strong reasoning capabilities through chain-of-thought mechanisms that generate step-by-step rationales. However, such slow-thinking approaches often lead to overthinking, where models produce excessively verbose responses even for simple queries, resulting in test-time inefficiency and even degraded accuracy. Prior work has attempted to mitigate this issue via adaptive reasoning strategies, but these methods largely overlook a fundamental bottleneck: visual perception failures. We argue that stable reasoning critically depends on low-level visual grounding, and that reasoning errors often originate from imperfect perception rather than insufficient deliberation. To address this limitation, we propose Gated Perception-Reasoning Optimization (GPRO), a meta-reasoning controller that dynamically routes computation among three decision paths at each generation step: a lightweight fast path, a slow perception path for re-examining visual inputs, and a slow reasoning path for internal self-reflection. To learn this distinction, we derive large-scale failure attribution supervision from approximately 790k samples, using teacher models to distinguish perceptual hallucinations from reasoning errors. We then train the controller with multi-objective reinforcement learning to optimize the trade-off between task accuracy and computational cost under uncertainty. Experiments on five benchmarks demonstrate that GPRO substantially improves both accuracy and efficiency, outperforming recent slow-thinking methods while generating significantly shorter responses.

## 1 Introduction

The reasoning capabilities of Large Vision-Language Models (LVLMs) have advanced considerably through chain-of-thought (CoT) and related techniques that encourage step-by-step problem decomposition (Wei et al., 2022; Kojima et al., 2022).

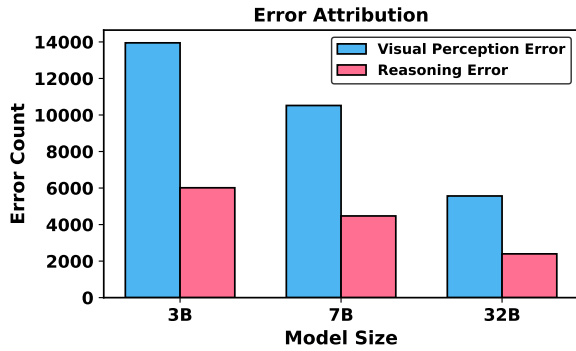


Figure 1: Error attribution of incorrect predictions from Qwen2.5-VL (Bai et al., 2025) across model scales. Results are based on about 790k samples from ViRL39k (Wang et al., 2025), MathV360K (Shi et al., 2024), and Mulberry (Yao et al., 2024a), and show that many errors stem from visual perception rather than reasoning.

This deliberate analytical approach enables models to solve complex mathematical and scientific problems by breaking them into manageable intermediate steps, and has proven effective across diverse domains, from arithmetic word problems to visually grounded scientific reasoning. However, applying such intensive computation uniformly across all inputs leads to a well-documented issue: overthinking. Models often generate verbose rationales for simple questions that could be answered directly, incurring test-time inefficiency and sometimes introducing errors through excessive elaboration (Kahneman, 2011).

Overthinking in LVLMs typically manifests in two patterns. First, models may produce redundant explanatory text that restates obvious visual information without advancing toward a solution (Zou et al., 2025). For instance, when asked to identify a clearly visible object’s color, a model may elaborate on the object’s shape, position, and context before stating the answer. This behavior is especially prevalent in models trained with extensive CoT data, where the training signal favors detailed explanations regardless of problem complexity. Second, models may engage in unnecessary reasoning

chains for problems that primarily require direct visual recognition. A simple counting question can trigger multi-step reasoning about spatial relations and numerical properties when straightforward enumeration would suffice.

Our analysis across multiple benchmarks shows that a substantial fraction of errors on challenging datasets arise from visual perception failures rather than from faulty reasoning (as illustrated in Figure 1). These failures occur when models misinterpret key visual cues before reasoning begins and are unlikely to be corrected by additional deliberation. This observation motivates our central thesis that adaptive computation in LVLMs should account for perceptual uncertainty alongside reasoning adaptation.

A key challenge in operationalizing this insight is the absence of supervision that distinguishes perceptual failures from reasoning errors. Standard benchmarks provide only final-answer correctness, offering no signal about which cognitive stage failed. To bridge this gap, we derive large-scale failure attribution supervision by mining incorrect predictions from approximately 790k samples spanning ViRL39k (Wang et al., 2025), MathV360K (Shi et al., 2024), and Mulberry (Yao et al., 2024a), and using stronger teacher models to attribute errors to perceptual hallucinations or reasoning failures. This supervision provides targeted signals for learning when additional perceptual or reasoning computation is warranted.

Building on this foundation, we introduce Gated Perception–Reasoning Optimization (GPRO), a framework that extends adaptive reasoning with targeted visual re-analysis. At its core, a meta-reasoning controller evaluates the model’s internal state at each token generation step and routes computation through one of three specialized paths: (1) a lightweight fast path for efficient direct generation; (2) a slow perception path that re-examines visual features to resolve perceptual uncertainty; and (3) a slow reasoning path that engages self-reflection to correct logical errors. This fine-grained control allocates computational resources precisely where they are needed, avoiding unnecessary deliberation while preserving robustness on challenging inputs.

The design of GPRO is inspired by cognitive science, where human problem solving combines fast intuitive responses with slower deliberative reasoning, alongside frequent re-inspection of perceptual inputs under uncertainty (Kahneman, 2011). By

explicitly supporting both perceptual re-analysis and reasoning self-correction, GPRO more closely mirrors this flexible cognitive process. Our contributions are summarized as follows:

- We identify visual perception failures as a critical bottleneck in LVLM performance, largely overlooked by existing adaptive reasoning methods.
- We derive large-scale failure attribution supervision from approximately 790k samples to distinguish perceptual hallucinations from reasoning errors.
- We propose the GPRO framework, which dynamically allocates computation between perception and reasoning at token-level granularity via a novel meta-reasoning controller.
- We demonstrate through extensive experiments on five benchmarks that GPRO models achieve strong accuracy with substantially reduced response lengths, establishing an effective approach for adaptive multimodal reasoning.

## 2 Related Work

### 2.1 Reasoning in Vision-Language Models

CoT prompting marked a significant advance in enhancing reasoning capabilities of large models (Wei et al., 2022). By generating step-by-step rationales before final answers, models can decompose complex problems into intermediate steps amenable to sequential processing. This paradigm has been extended to multimodal settings, where LVLMs generate interleaved text and visual analysis to solve reasoning problems (Liu et al., 2024; Bai et al., 2025). The key insight is that explicit intermediate steps allow models to leverage their language modeling capabilities for multi-hop reasoning that would be difficult in a single forward pass.

Subsequent work has refined this process through various mechanisms. Self-correction approaches (Madaan et al., 2024) enable models to identify and fix errors in their own reasoning paths through iterative refinement. Tree of Thoughts (Yao et al., 2024b) explores multiple reasoning paths simultaneously, enabling backtracking and alternative solution exploration when initial approaches fail. These methods have pushed performance boundaries on complex reasoning tasks but often incur substantial computational overhead.

Recent models have demonstrated increasingly sophisticated reasoning capabilities. Mulberry

(Yao et al., 2024a) achieves o1-like reasoning through collective Monte Carlo tree search, enabling systematic exploration of solution spaces. Virgo (Du et al., 2025) explores reproducing slow-thinking mechanisms in multimodal settings through careful data curation and training procedures. LMM-R1 (Peng et al., 2025) employs two-stage rule-based reinforcement learning to enhance reasoning in smaller models. These approaches represent important progress but share a common limitation: they focus primarily on reasoning depth without explicitly addressing perceptual accuracy.

## 2.2 Efficiency and Adaptive Computation

The computational cost of exhaustive reasoning has spurred research on adaptive computation strategies. Mixture-of-Experts architectures (Shazeer et al., 2017; Fedus et al., 2022) selectively activate parameter subsets based on input characteristics, enabling capacity scaling without proportional cost increases for every input. The sparse activation pattern provides a natural mechanism for adaptive computation, as different experts can specialize in different input types or reasoning patterns.

Early-exit mechanisms and model cascades represent another approach, routing simpler queries through lightweight processing paths while reserving full model capacity for complex inputs. These methods recognize that not all inputs require the same computational depth and that significant efficiency gains are possible through intelligent routing. Recent work has explored adaptive reasoning strategies specifically for vision-language models. The FAST framework (Xiao et al., 2025) investigates how response length and data distribution affect LVLM performance, developing methods to dynamically adjust reasoning depth based on problem characteristics. Vision-R1 (Huang et al., 2025) incentivizes reasoning capability through reinforcement learning on curated multimodal CoT data. Curr-ReFT (Deng et al., 2025a) proposes curriculum reinforcement finetuning to address training bottlenecks in smaller VLMs. Our work extends this direction by explicitly incorporating perceptual uncertainty alongside reasoning adaptation.

## 2.3 Reinforcement Learning for Language Models

Reinforcement learning has become central to training adaptive computation frameworks and aligning model behavior with desired objectives. Proximal Policy Optimization (Schulman et al., 2017) and re-

lated algorithms enable models to optimize policies balancing multiple objectives such as accuracy and efficiency. Reinforcement Learning from Human Feedback (Ouyang et al., 2022) has proven effective for aligning model behavior with human preferences, demonstrating that RL can shape complex behaviors difficult to specify through supervised learning alone.

Recent multimodal reasoning models have applied RL-based approaches with notable success. R1-OneVision (Yang et al., 2025) advances generalized multimodal reasoning through cross-modal formalization trained with reinforcement learning. MM-Eureka (Meng et al., 2025) explores rule-based reinforcement learning for multimodal reasoning at scale. OpenVLThinker (Deng et al., 2025b) demonstrates that iterative self-improvement through alternating supervised finetuning and reinforcement learning can yield sophisticated CoT reasoning capabilities.

Our GPRO framework employs a similar RL-based approach but introduces a more sophisticated state representation incorporating visual perception signals alongside reasoning uncertainty. This enables the controller to trigger dedicated visual re-analysis when perceptual uncertainty is high, a capability absent from prior adaptive reasoning methods that focus solely on reasoning depth.

## 3 Method

We introduce Gated Perception-Reasoning Optimization (GPRO), a framework that augments standard LVLMs with dynamic, fine-grained control over computational resource allocation. The key innovation is a Gated Perception-Reasoning (GPR) module that replaces selected feed-forward layers in the decoder, enabling token-level decisions about whether to invoke additional perception or reasoning computation.

### 3.1 Gated Perception-Reasoning Architecture

The GPR module serves as a lightweight replacement for standard FFN layers, strategically inserted at alternating positions in the Transformer decoder to balance adaptive computation with base model capabilities. This alternating pattern ensures the model maintains its foundational representational power while gaining flexibility to dynamically adjust its computational strategy. Each GPR module comprises a meta-reasoning controller and three computational paths, as illustrated in Figure 2.

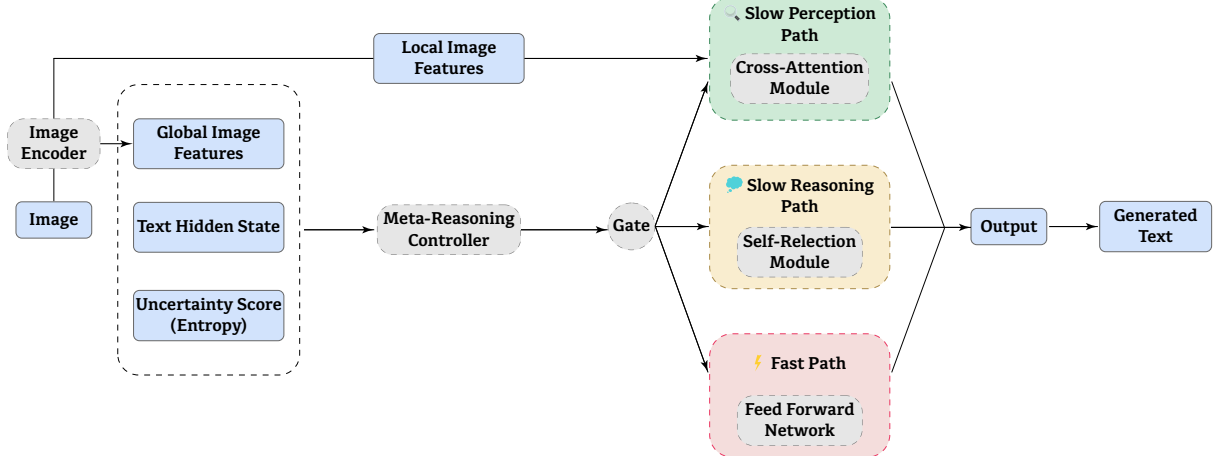


Figure 2: GPRO architecture overview. The meta-reasoning controller receives text hidden states, uncertainty scores, and global image features to route among Fast Path (FFN), Slow Perception Path (Cross-Attention), and Slow Reasoning Path (Self-Reflection).

### 3.1.1 Meta-Reasoning Controller

The controller is a compact 2-layer Transformer that determines path selection for each generated token. Its lightweight design ensures minimal overhead while providing sufficient capacity for nuanced decision-making. At timestep  $t$ , the controller receives a state vector  $s_t$  that encapsulates the model’s current cognitive state through three complementary signals.

The first signal is the current hidden state  $h_t$  from the main decoder, encoding the semantic context of generated text. This captures what the model knows at the current generation step and provides information about the reasoning trajectory so far. The second signal is an uncertainty score  $U_t$  computed as predictive entropy over output logits, quantifying the model’s confidence in its next token prediction. High entropy indicates the model is uncertain about how to proceed, suggesting additional computation may be beneficial. The third signal is global image features  $V_g$  summarizing the visual context, providing the controller with information about the visual input’s complexity and content.

Based on the concatenated state  $s_t = [h_t; U_t; V_g]$ , the controller outputs a discrete action  $a_t \in \{\text{fast, perception, reasoning}\}$  selecting one of three computational paths.

### 3.1.2 Computational Paths

The three paths address distinct computational needs arising during generation:

**Fast Path.** The default low-cost option utilizing the original FFN layer from the base model. This path is selected when the model is confident in

both its perceptual understanding and reasoning trajectory:

$$\text{Fast}(h_t) = \text{GELU}(h_t W_1 + b_1) W_2 + b_2. \quad (1)$$

The fast path preserves the base model’s efficient generation capability for straightforward cases.

**Slow Perception Path.** Activated when the controller detects high perceptual uncertainty, this path uses the current hidden state as a query for cross-attention over visual features:

$$\text{Perc}(h_t, V) = \text{CrossAttn}(h_t, V, V). \quad (2)$$

This enables the model to re-examine the image, focusing on details relevant to current generation. The cross-attention mechanism allows targeted retrieval of visual information that may have been overlooked or misinterpreted in initial processing.

**Slow Reasoning Path.** Engaged when logical uncertainty is high, this path passes the current hidden state and recent context to a meta-reasoning module:

$$\text{Reas}(h_t, H_{<t}) = \text{MetaTrans}(h_t, H_{<t}). \quad (3)$$

This supports internal self-reflection, allowing the model to reconsider its reasoning trajectory without generating additional output tokens. The reasoning path can identify and correct logical errors before they propagate to subsequent generation steps.

## 3.2 Multi-Objective Training

The meta-reasoning controller is trained via PPO-based reinforcement learning with a multi-

Field	Description
id	Unique identifier of the sample (e.g., <code>mathv360k_mathv_219220</code> )
image	Relative path to the associated image file (e.g., <code>images/413164.jpg</code> )
conversations	Multi-turn dialogue represented as a list of (role, content) pairs. The user input may contain an image token (<image>).
meta_info.source	Original dataset source (e.g., MathV360K).
meta_info.sample_type	Sample label indicating correctness or usability (e.g., <code>positive</code> ).
meta_info.difficulty	Estimated difficulty level of the sample (e.g., <code>medium</code> ).
meta_info.original_entropy	Entropy of the model prediction distribution before dataset filtering.
meta_info.failure_reason	Failure category for incorrect samples; <code>None</code> for successful samples.

Table 1: Metadata schema for the derived failure attribution supervision.

objective reward function designed to balance competing desiderata:

$$R(\tau) = R_{\text{task}} + \alpha_c R_{\text{cost}} + \alpha_l R_{\text{cal}}, \quad (4)$$

where  $\alpha_c$  and  $\alpha_l$  are weighting coefficients controlling the trade-off between accuracy and efficiency.

**Task Reward.** A sparse signal providing the primary learning signal:  $R_{\text{task}} = +1$  for correct final answers, 0 otherwise. This ensures the model prioritizes accuracy as its primary objective.

**Cost Reward.** Penalizes activation of computationally expensive slow paths:

$$R_{\text{cost}} = - \sum_t (c_p \mathbb{1}_{[a_t=p]} + c_r \mathbb{1}_{[a_t=r]}), \quad (5)$$

where  $c_p$  and  $c_r$  are cost coefficients for perception and reasoning paths respectively. This encourages reliance on the fast path when additional computation is unnecessary.

**Calibration Reward.** Ensures uncertainty scores reliably indicate when slow paths are needed:

$$R_{\text{cal}} = - \sum_{t \in \mathcal{E}} (1 - U_t) - \sum_{t \in \mathcal{C}} U_t, \quad (6)$$

where  $\mathcal{E}$  and  $\mathcal{C}$  denote tokens leading to incorrect and correct answers respectively. This reward encourages the model to be uncertain when it should be (before errors) and confident when it should be (before correct outputs), enabling the controller to make well-informed decisions.

### 3.3 Training Data Construction

Effective training of the controller requires data that exposes both perceptual and reasoning failure modes. We construct such data through a systematic three-step procedure.

First, we perform failure case mining by running Qwen2.5-VL on a combined dataset of approximately 790K samples from ViRL39k (Wang et al.,

2025), MathV360K (Shi et al., 2024), and Mulberry (Yao et al., 2024a), collecting all instances where the model produces incorrect answers. This provides a rich set of failure cases spanning diverse visual reasoning challenges.

Second, we conduct failure attribution using GPT-4 to categorize each failure as either a visual perception failure or reasoning error propagation. The categorization is based on analysis of the question, image, incorrect answer, and ground truth. Visual perception failures are identified when the model’s error can be traced to a misinterpretation of visual elements, while reasoning errors are identified when visual understanding appears correct but the logical steps are flawed. The metadata schema of the derived failure attribution supervision is shown in Table 1.

Third, we construct a training curriculum from the labeled data, oversampling difficult examples to ensure the controller encounters sufficient instances of both failure types. For the 3B model, we curate approximately 40K training samples, while the 7B model uses approximately 30K samples. The smaller sample size for the larger model reflects its stronger base capabilities requiring less corrective training.

## 4 Experiments

We evaluate GPRO on five challenging benchmarks to address three questions: (1) How does GPRO compare to state-of-the-art methods in accuracy and efficiency? (2) What are the contributions of individual components? (3) How does the model behave qualitatively?

### 4.1 Experimental Setup

**Baselines.** We compare against three categories of baselines. Closed-source models include GPT-4o (Hurst et al., 2024), Claude-3.5 Sonnet (Anthropic, 2024), and Qwen-VL-Max (Bai et al.,

Method	MathVision		MathVerse		MathVista		DynaMath		MM-Vet	
	Acc.	Len.								
<i>Closed-Source Models</i>										
GPT-4o (Hurst et al., 2024)	30.4	–	<b>49.9</b>	–	63.8	–	<u>63.7</u>	–	<b>80.8</b>	–
Claude-3.5 Sonnet (Anthropic, 2024)	<u>37.9</u>	–	46.3	–	<u>67.7</u>	–	<b>64.8</b>	–	68.7	–
Qwen-VL-Max (Bai et al., 2023)	<b>39.3</b>	–	<u>47.3</u>	–	<b>74.2</b>	–	–	–	<u>73.2</u>	–
<i>Base Qwen2-VL-7B</i>										
Qwen2-VL-7B (Wang et al., 2024b)	18.8	443.0	31.9	388.9	<b>58.2</b>	<b>265.9</b>	39.8	298.4	<b>62.0</b>	<b>132.5</b>
Mulberry (Yao et al., 2024a)	<u>23.4</u>	<b>349.2</b>	<b>39.5</b>	<b>364.3</b>	<b>62.1</b>	<u>275.0</u>	<b>46.8</b>	<b>273.3</b>	<u>43.9</u>	<u>218.3</u>
Virgo (Du et al., 2025)	<b>24.0</b>	–	<u>36.7</u>	–	–	–	–	–	–	–
<i>Base Qwen2.5-VL-3B</i>										
Qwen2.5-VL-3B (Bai et al., 2025)	21.2	450.6	34.6	362.3	62.3	212.9	48.2	270.9	61.3	138.8
Curr-ReFT (Deng et al., 2025a)	20.1	<b>240.1</b>	36.3	<b>121.6</b>	61.9	<b>95.9</b>	43.8	<b>146.4</b>	62.0	117.6
LMM-R1 (Peng et al., 2025)	25.2	447.8	41.8	423.9	63.2	245.0	53.1	341.6	<b>65.9</b>	166.3
FAST-3B (Xiao et al., 2025)	<u>26.8</u>	323.5	<u>43.0</u>	286.3	<u>66.2</u>	158.7	<u>54.4</u>	213.7	64.0	<u>112.7</u>
<b>GPRO-3B (Ours)</b>	<b>27.1</b>	<b>298.6</b>	<b>44.2</b>	<u>265.4</u>	<b>66.8</b>	<u>145.2</u>	<b>55.1</b>	<u>195.3</u>	<u>65.2</u>	<b>108.4</b>
<i>Base Qwen2.5-VL-7B</i>										
Qwen2.5-VL-7B (Bai et al., 2025)	25.6	443.0	46.9	388.9	68.2	189.1	58.0	273.3	67.1	132.5
MM-R1 (Liang et al., 2025)	30.2	324.6	<b>49.8</b>	283.9	71.0	185.6	57.5	254.2	70.6	137.9
Vision-R1 (Huang et al., 2025)	–	–	52.4	–	73.5	–	–	–	–	–
R1-OneVision (Yang et al., 2025)	29.9	692.8	46.4	631.5	64.1	402.5	53.5	560.6	<b>71.6</b>	440.7
OpenVLThinker (Deng et al., 2025b)	29.6	457.2	47.9	398.4	70.2	305.7	57.4	382.1	68.5	312.7
FAST-7B (Xiao et al., 2025)	<u>30.6</u>	<u>204.8</u>	<b>50.6</b>	<u>201.0</u>	<u>73.8</u>	<u>120.7</u>	<u>58.3</u>	<u>164.8</u>	<u>71.2</u>	<b>114.1</b>
<b>GPRO-7B (Ours)</b>	<b>31.2</b>	<b>195.6</b>	48.7	<b>188.4</b>	<b>74.2</b>	<b>115.3</b>	<b>59.2</b>	<b>158.7</b>	70.9	<u>118.8</u>

Table 2: Main results on five reasoning benchmarks. We report accuracy (%) and average response length (tokens). Response lengths are measured using Qwen2.5-VL’s tokenizer. **Bold** results indicate the best performance among all methods, while underlined results indicate the second-best performance among all methods.

2023), representing current commercial capabilities. Base models include Qwen2-VL-7B (Wang et al., 2024b) and Qwen2.5-VL (Bai et al., 2025) at 3B and 7B scales. Recent slow-thinking methods include Mulberry (Yao et al., 2024a), Virgo (Du et al., 2025), Curr-ReFT (Deng et al., 2025a), LMM-R1 (Peng et al., 2025), MM-R1 (Liang et al., 2025), Vision-R1 (Huang et al., 2025), R1-OneVision (Yang et al., 2025), OpenVLThinker (Deng et al., 2025b), and FAST (Xiao et al., 2025).

**Benchmarks.** We evaluate on five benchmarks requiring sophisticated visual and mathematical reasoning: MathVision (Wang et al., 2024a) for geometric and mathematical problems in visual contexts; MathVerse (Zhang et al., 2024) for mathematical reasoning with complex visual diagrams; MathVista (Lu et al., 2024) covering diverse mathematical reasoning grounded in visual information; DynaMath (Zou et al., 2024) for dynamic mathematical reasoning; and MM-Vet (Yu et al., 2023) for integrated multimodal capabilities.

**Implementation.** GPRO models are built on Qwen2.5-VL with GPR modules replacing alternate FFN layers. Training used 8 NVIDIA H100 GPUs with batch size 512, 8 rollouts per question, for 10 epochs (approximately 600 GPU hours). Re-

ward weights were  $\alpha_c = 0.1$ ,  $\alpha_l = 0.2$ , with learning rate  $1 \times 10^{-5}$  and cosine decay schedule.

## 4.2 Main Results

Table 2 presents a comprehensive comparison across five multimodal reasoning benchmarks. We report both accuracy (%) and average response length (tokens) to facilitate a dual analysis of performance and computational efficiency.

The empirical results in Table 2 reveal several critical insights regarding the interplay between reasoning depth and computational efficiency.

**Optimizing the Efficiency-Accuracy Frontier.** First and foremost, GPRO consistently redefines the Pareto frontier for multimodal reasoning. Unlike prior methods that trade inference speed for accuracy, our approach achieves superior performance while dramatically curtailing token generation. On MathVerse, GPRO-7B improves accuracy by 1.8% over the base Qwen2.5-VL-7B while reducing the average response length by 51.5% (from 388.9 to 188.4 tokens). Similarly, on MathVista, we observe a 6.0% accuracy gain alongside a 39% reduction in tokens. This confirms our core hypothesis: model performance is not strictly proportional to generation length, and intelligent resource allocation can mitigate the overthinking phenomenon

inherent in standard CoT processes.

**Critique of Unconditional Long-Context Reasoning.** A comparison with recent long-CoT distillation models, such as R1-OneVision and OpenVLThinker, highlights the limitations of unconditional slow thinking. R1-OneVision exhibits extreme token consumption (e.g., 692.8 tokens on MathVision) yet often underperforms our method (29.9% vs. 31.2% for GPRO-7B). This suggests that forcing models to generate extensive reasoning paths for every query introduces noise or hallucination rather than clarity. GPRO’s selective activation mechanism acts as a surgical intervention, allocating computational budget only when necessary, thereby achieving a  $\sim 3.5 \times$  reduction in inference cost compared to R1-OneVision while surpassing its accuracy.

**Competitiveness with Proprietary Giants.** Notably, GPRO-7B demonstrates surprising resilience against closed-source models orders of magnitude larger. On MathVision, GPRO-7B (31.2%) outperforms GPT-4o (30.4%), and on MathVista, it matches the performance of Qwen-VL-Max (74.2%). This result is significant as it indicates that smaller, open-weights models, when equipped with efficient meta-reasoning strategies, can bridge the gap with proprietary SOTA models in specific reasoning-heavy domains.

**Scalability Across Model Sizes.** Finally, the benefits of GPRO are robust across model scales. GPRO-3B outperforms the strong FAST-3B baseline on 4 out of 5 benchmarks and substantially improves upon the base Qwen2.5-VL-3B (e.g., +9.6% on MathVerse). This scalability suggests that the perception-reasoning decomposition is a fundamental improvement applicable to various architectures, rather than a parameter-scale-dependent optimization. The consistent gains in both the 3B and 7B settings validate the universality of our proposed controller mechanism.

### 4.3 Ablation Study

To deconstruct the efficacy of GPRO and isolate the impact of its constituent modules, we conducted a component-wise ablation study. Table 3 summarizes the performance contributions of the Slow Perception path, Slow Reasoning path, and the Calibration Reward mechanism.

**Dominance of Visual Grounding.** The most significant performance degradation occurs upon re-

Configuration	MathVision	MathVerse
<b>Full GPRO-7B</b>	<b>31.2</b>	<b>48.7</b>
w/o Slow Perception	27.8 (-3.4)	44.3 (-4.4)
w/o Slow Reasoning	29.5 (-1.7)	47.0 (-1.7)
w/o Calibration Reward	28.9 (-2.3)	46.2 (-2.5)

Table 3: Ablation study results on MathVision and MathVerse. Numbers in parentheses indicate the absolute accuracy drop compared to the full model configuration.

moving the *Slow Perception Path*, resulting in a sharp decline of 3.4% on MathVision and 4.4% on MathVerse. This finding empirically validates our core hypothesis: visual hallucinations serve as the primary bottleneck in multimodal reasoning. When the model is deprived of the mechanism to re-examine visual features, initial perceptual errors (e.g., misreading axis scales or misidentifying geometric primitives) propagate irreversibly through the reasoning chain. The disparity between the perception drop (-4.4%) and the reasoning drop (-1.7%) highlights that current VLMs suffer more from "garbage-in" perceptual failures than from logical deduction errors.

**Role of Reflexive Reasoning.** The *Slow Reasoning Path*, while less critical than perception, contributes a consistent improvement ( $\sim 1.7\%$  across benchmarks). This module effectively mitigates logic-level errors by enabling self-correction during complex multi-step derivations. However, its lower relative impact suggests that the base Qwen2.5 model possesses robust inherent reasoning capabilities, and the marginal gain from "thinking longer" is diminishing unless grounded in accurate visual data.

**Importance of Uncertainty Calibration.** Abolishing the *Calibration Reward* leads to a substantial performance drop (2.3%–2.5%), underscoring the necessity of alignment between the controller’s confidence and task difficulty. Without this reward signal, the meta-controller fails to learn an optimal switching policy, often collapsing into a mode of either indiscriminate fast-path usage (under-thinking) or wasteful slow-path activation (over-thinking). The calibration reward effectively regularizes the decision boundary, ensuring that computational overhead is incurred only when model uncertainty is genuinely indicative of potential failure.

**Resource Allocation Dynamics.** To further understand the controller’s behavior, we analyze the path activation distribution on the MathVision test

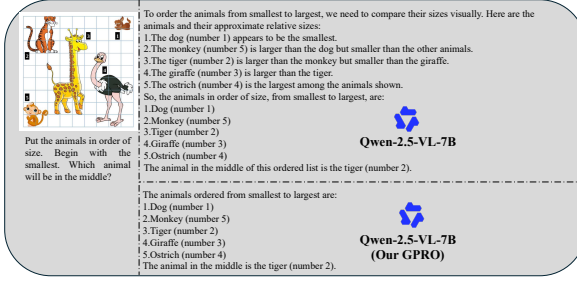


Figure 3: Case Study 1: Animal size ordering. The baseline produces verbose step-by-step comparisons, while GPRO generates a concise direct answer.

set. As illustrated in the distribution analysis, GPRO-7B activates the Fast Path for 73% of tokens, allocating the Slow Perception Path (17%) and Slow Reasoning Path (10%) sparsely. This highly skewed distribution confirms that the model has learned a resource-efficient policy, treating slow thinking as a surgical intervention rather than a default mode. Qualitative inspection reveals that Slow Perception is triggered predominantly on high-frequency visual tokens (e.g., numbers in tables, coordinates, legend texts), whereas Slow Reasoning activates during transitional logical connectives (e.g., "therefore", "implies"), demonstrating the semantic awareness of our learned controller.

#### 4.4 Case Study

We present two case studies to illustrate how GPRO mitigates overthinking while preserving accuracy through adaptive resource allocation.

**Case 1: Visual Ordering Task.** Figure 3 depicts a task that requires ordering animals by size and identifying the middle one. The baseline Qwen2.5-VL-7B produces lengthy explanations for each animal's relative size (e.g., "the dog appears to be the smallest," "the monkey is larger than the dog but smaller than the other animals") before arriving at the answer. This behavior exemplifies overthinking, where detailed reasoning is applied to a task that primarily depends on visual perception. In contrast, GPRO identifies this as a straightforward visual task and predominantly relies on the Fast Path, with selective activation of the Slow Perception Path to verify size relationships when ambiguity arises. As a result, GPRO produces a correct and concise answer, identifying the tiger as the middle animal while generating substantially fewer tokens.

**Case 2: Spatial Reasoning.** Figure 4 presents a more complex spatial reasoning task that involves counting the number of black cubes required to make a larger cube opaque from all viewing direc-

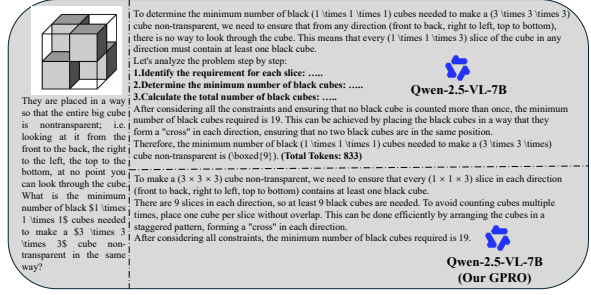


Figure 4: Case Study 2: Spatial reasoning with cubes. The baseline generates 833 tokens of detailed analysis, while GPRO produces an efficient solution.

tions. The baseline generates 833 tokens of step-by-step analysis, explicitly enumerating constraints for each slice and direction before reaching a conclusion. GPRO, in contrast, selectively activates the Slow Perception Path to accurately interpret the 3D structure shown in the image, followed by the Slow Reasoning Path to verify the counting logic. The model correctly identifies the key constraint that each slice along every direction must contain at least one black cube, and arrives at the correct answer with significantly fewer tokens. This example illustrates how GPRO coordinates perception and reasoning by invoking additional computation only when needed, leading to a correct solution with substantially reduced generation length.

Together, these cases demonstrate the core advantage of GPRO: dynamically allocating computation based on task demands, avoiding unnecessary verbosity for simple inputs while engaging deeper analysis only when required.

## 5 Conclusion

We introduce Gated Perception–Reasoning Optimization (GPRO), a gated adaptive computation framework for LVLMs. This work is motivated by the observation that visual perception failures constitute a critical yet underexplored bottleneck in LVLM performance. Such failures often co-occur with overthinking and limit the effectiveness of deeper reasoning alone. GPRO leverages failure attribution supervision to distinguish perceptual errors from reasoning errors, and uses this signal to guide a meta-reasoning controller that routes token-level generation among fast execution, visual re-examination, and reasoning refinement. Experiments on five challenging benchmarks show that GPRO improves accuracy while consistently reducing response length, demonstrating an effective approach to adaptive multimodal reasoning.

## 6 Limitations

While GPRO demonstrates strong effectiveness on vision–language reasoning benchmarks, several limitations remain.

First, our current formulation and evaluation focus on static vision–language inputs. The core idea of separating perception and reasoning uncertainty is modality-agnostic and could naturally extend to other modalities such as audio and video, where similar perception–reasoning trade-offs may arise.

Second, GPRO adopts a discrete routing scheme over a fixed set of computation paths. Exploring finer-grained or continuous control over perception and reasoning interventions may offer additional flexibility, which we leave to future work.

## Ethical Considerations

All experiments presented in this study were conducted using publicly available datasets and models licensed for academic research purposes. To the best of our knowledge, this work does not present any ethical concerns.

## References

Anthropic. 2024. *The claude 3 model family: Opus, sonnet, haiku*.

Jinze Bai, Shuai Bai, Shusheng Yang, Shijie Wang, Sinan Tan, Peng Wang, Junyang Lin, Chang Zhou, and Jingren Zhou. 2023. *Qwen-vl: A versatile vision-language model for understanding, localization, text reading, and beyond*. *arXiv preprint arXiv:2308.12966*.

Shuai Bai, Keqin Chen, Xuejing Liu, Jialin Wang, Wenbin Ge, Sibo Song, Kai Dang, Peng Wang, Shijie Wang, Jun Tang, and 1 others. 2025. *Qwen2. 5-vl technical report*. *arXiv preprint arXiv:2502.13923*.

Huilin Deng, Hongchen Shi, Yicheng Zhu, Junfeng Yin, Shen Zheng, Zilong Liu, and 1 others. 2025a. *Boosting the generalization and reasoning of vision language models with curriculum reinforcement learning*. *arXiv preprint arXiv:2503.07065*.

Yihe Deng, Hritik Bansal, Fan Yin, Nanyun Peng, Wei Wang, and Kai-Wei Chang. 2025b. *Openvlthinker: An early exploration to complex vision-language reasoning via iterative self-improvement*. *arXiv preprint arXiv:2503.17352*.

Yifan Du, Zikang Li, Yifan Ding, Junyu Feng, Xinyu Zuo, Xudong Zhao, Longteng Tian, Rui Zheng, Zhaopeng Wen, Minlie Huang, and 1 others. 2025. *Virgo: A preliminary exploration on reproducing o1-like mllm*. *arXiv preprint arXiv:2501.01904*.

William Fedus, Barret Zoph, and Noam Shazeer. 2022. *Switch transformers: Scaling to trillion parameter models with simple and efficient sparsity*. *Journal of Machine Learning Research*.

Wenyi Huang, Bohan Jia, Zijie Zhai, Zhiqi Cai, Shaobin Gao, Zhi Wang, Luoyi Chen, and 1 others. 2025. *Vision-r1: Incentivizing reasoning capability in multimodal large language models*. *arXiv preprint arXiv:2503.06749*.

Aaron Hurst, Adam Lerer, Adam P Goucher, Adam Perelman, Aditya Ramesh, Aidan Clark, AJ Ostrow, Akila Welihinda, Alan Hayes, Alec Radford, and 1 others. 2024. *Gpt-4o system card*. *arXiv preprint arXiv:2410.21276*.

Daniel Kahneman. 2011. *Thinking, Fast and Slow*. Farrar, Straus and Giroux.

Takeshi Kojima, Shixiang Shane Gu, Machel Reid, Yutaka Matsuo, and Yusuke Iwasawa. 2022. *Large language models are zero-shot reasoners*. In *Advances in Neural Information Processing Systems*.

Qiankun Liang, Yuxuan Chen, Ziming Liu, Shaobin Huang, and 1 others. 2025. *Mm-r1: Unleashing the power of unified multimodal large language models for personalized image generation*. *arXiv preprint arXiv:2508.11433*.

Haotian Liu, Chunyuan Li, Qingyang Wu, and Yong Jae Lee. 2024. *Visual instruction tuning*. In *Advances in Neural Information Processing Systems*.

Pan Lu, Hritik Bansal, Tony Xia, Jiacheng Liu, Chunyuan Li, Hannaneh Hajishirzi, Hao Cheng, Kai-Wei Chang, Michel Galley, and Jianfeng Gao. 2024. *Mathvista: Evaluating mathematical reasoning of foundation models in visual contexts*. *arXiv preprint arXiv:2310.02255*.

Aman Madaan, Niket Tandon, Prakhar Gupta, Skyler Hallinan, Luyu Gao, Sarah Wiegreffe, Uri Alon, Nouha Dziri, Shrimai Prabhumoye, Yiming Yang, and 1 others. 2024. *Self-refine: Iterative refinement with self-feedback*. *Advances in Neural Information Processing Systems*.

Fanqing Meng, Lingxiao Du, Zongkai Liu, Zhixiang Zhou, Quanfeng Lu, Daocheng Fu, Tiancheng Han, Botian Shi, Wenhui Wang, Junjun He, and 1 others. 2025. *Mm-eureka: Exploring the frontiers of multimodal reasoning with rule-based reinforcement learning*. *arXiv preprint arXiv:2503.07365*.

Long Ouyang, Jeffrey Wu, Xu Jiang, Diogo Almeida, Carroll Wainwright, Pamela Mishkin, Chong Zhang, Sandhini Agarwal, Katarina Slama, Alex Ray, and 1 others. 2022. *Training language models to follow instructions with human feedback*. In *Advances in Neural Information Processing Systems*.

Yingzhe Peng, Gongrui Liu, Cheng Zhang, Haoran Xu, Jiawei Liu, Xin Li, Ning Ding, Yu Qiao, Jie Liu, and 1 others. 2025. *Lmm-r1: Empowering 3b lmms*.

with strong reasoning abilities through two-stage rule-based rl. *arXiv preprint arXiv:2503.07536*.

John Schulman, Filip Wolski, Prafulla Dhariwal, Alec Radford, and Oleg Klimov. 2017. **Proximal policy optimization algorithms**. *arXiv preprint arXiv:1707.06347*.

Noam Shazeer, Azalia Mirhoseini, Krzysztof Maziarz, Andy Davis, Quoc Le, Geoffrey Hinton, and Jeff Dean. 2017. **Outrageously large neural networks: The sparsely-gated mixture-of-experts layer**. *arXiv preprint arXiv:1701.06538*.

Wenhai Shi, Zhiqiang Hu, Yi Bin, Junhua Liu, Yang Yang, See Kiong Ng, Lidong Bing, and Roy Ka-Wei Lee. 2024. **Math-llava: Bootstrapping mathematical reasoning for multimodal large language models**. In *Findings of the Association for Computational Linguistics: EMNLP 2024*.

Haozhe Wang, Chao Qu, Zuming Huang, Wei Chu, Fangzhen Lin, and Wenhui Chen. 2025. **VL-rethinker: Incentivizing self-reflection of vision-language models with reinforcement learning**. *arXiv preprint arXiv:2504.08837*.

Ke Wang, Junting Wang, Jingyi Shao, Zimu Shi, Wenya Guan, Weijie Liu, Xuefeng Wang, and Rui Zhong. 2024a. **Measuring multimodal mathematical reasoning with math-vision dataset**. *arXiv preprint arXiv:2402.14804*.

Peng Wang, Shuai Bai, Sinan Tan, Shijie Wang, Zhihao Fan, Jinze Bai, Keqin Chen, Xuejing Liu, Jialin Wang, Wenbin Ge, and 1 others. 2024b. **Qwen2-vl: Enhancing vision-language model's perception of the world at any resolution**. *arXiv preprint arXiv:2409.12191*.

Jason Wei, Xuezhi Wang, Dale Schuurmans, Maarten Bosma, Brian Ichter, Fei Xia, Ed Chi, Quoc Le, and Denny Zhou. 2022. **Chain-of-thought prompting elicits reasoning in large language models**. In *Advances in Neural Information Processing Systems*.

Wenyi Xiao, Lin Gan, Wanggui Dai, Wenhao He, Zizwei Huang, Haoyuan Li, Yichao Zhu, Wentao Zhu, Ruofan Jiang, Weijia Shao, and 1 others. 2025. **Fast-slow thinking grp for large vision-language model reasoning**. *arXiv preprint arXiv:2504.18458*.

Yi Yang, Xiaocui Yin, Shuo Wang, Yifu Chen, Yingying Li, Wenjie Wang, Yuhao Zhong, Jiaqi Deng, and 1 others. 2025. **R1-onevision: Advancing generalized multimodal reasoning through cross-modal formalization**. *arXiv preprint arXiv:2503.10615*.

Huanjin Yao, Jiaxing Wu, Wenhao Wang, Jingyi Dong, Yibo Liang, Shunyu Zhu, Yingjie Wang, Yuxin Tan, Haoran Liu, Jianye Wang, and 1 others. 2024a. **Mulberry: Empowering mllm with o1-like reasoning and reflection via collective monte carlo tree search**. *arXiv preprint arXiv:2412.18319*.

Shunyu Yao, Dian Yu, Jeffrey Zhao, Izhak Shafran, Thomas L Griffiths, Yuan Cao, and Karthik Narasimhan. 2024b. **Tree of thoughts: Deliberate problem solving with large language models**. In *Advances in Neural Information Processing Systems*.

Weihao Yu, Zhengyuan Yang, Linjie Li, Jianfeng Wang, Kevin Lin, Zicheng Liu, Xinchao Wang, and Lijuan Wang. 2023. **Mm-vet: Evaluating large multimodal models for integrated capabilities**. *arXiv preprint arXiv:2308.02490*.

Renrui Zhang, Dongzhi Jiang, Yichi Zhang, Haokun Lin, Ziyu Guo, Pengshuo Qiu, Aojun Zhou, Pan Lu, Kai-Wei Chang, Peng Gao, and 1 others. 2024. **Mathverse: Does your multi-modal llm truly see the diagrams in visual math problems?** *arXiv preprint arXiv:2403.14624*.

Chengke Zou, Xingang Zhang, Rui Zhao, Wei Li, Junchi Guo, and Wentao Zhu. 2024. **Dynamath: A dynamic visual benchmark for evaluating mathematical reasoning robustness of vision language models**. *arXiv preprint arXiv:2411.00836*.

Xin Zou, Yizhou Wang, Yibo Yan, Yuanhuiyi Lyu, Kening Zheng, Sirui Huang, Junkai Chen, Peijie Jiang, Jia Liu, Chang Tang, and Xuming Hu. 2025. **Look twice before you answer: Memory-space visual re-tracing for hallucination mitigation in multimodal large language models**. In *International Conference on Machine Learning*.